Chemical Research in Toxicology

Subscriber access provided by University of Washington | Libraries

Article

In Vitro Metabolism and Covalent Binding of Enol-Carboxamide Derivatives and Anti-Inflammatory Agents Sudoxicam and Meloxicam: Insights into the Hepatotoxicity of Sudoxicam

R. Scott Obach, Amit S. Kalgutkar, Tim F. Ryder, and Gregory S. Walker

Chem. Res. Toxicol., **2008**, 21 (9), 1890-1899• DOI: 10.1021/tx800185b • Publication Date (Web): 16 August 2008

Downloaded from http://pubs.acs.org on April 27, 2009

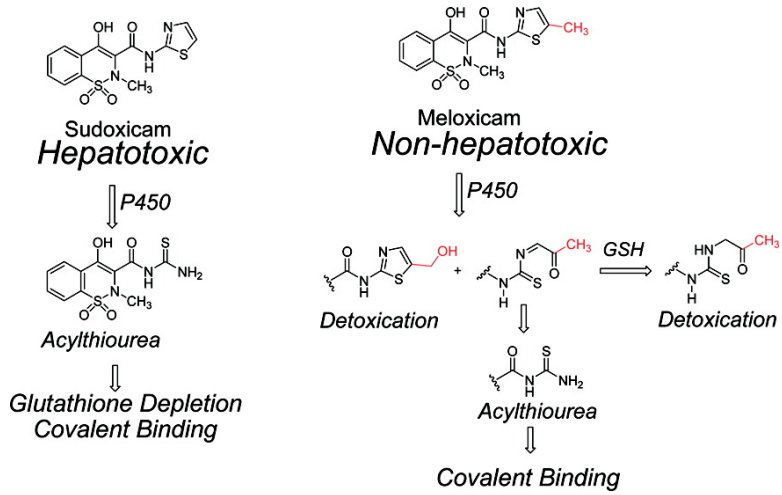

More About This Article

Additional resources and features associated with this article are available within the HTML version:

- Supporting Information
- Links to the 1 articles that cite this article, as of the time of this article download
- Access to high resolution figures
- Links to articles and content related to this article
- Copyright permission to reproduce figures and/or text from this article

View the Full Text HTML

ACS Publications
High quality. High impact.

Chemical Research in Toxicology is published by the American Chemical Society.
1155 Sixteenth Street N.W., Washington, DC 20036

In Vitro Metabolism and Covalent Binding of Enol-Carboxamide Derivatives and Anti-Inflammatory Agents Sudoxicam and Meloxicam: Insights into the Hepatotoxicity of Sudoxicam

R. Scott Obach,* Amit S. Kalgutkar, Tim F. Ryder, and Gregory S. Walker

Pharmacokinetics, Dynamics, and Metabolism Department, Pfizer Global Research and Development, Groton, Connecticut

Received May 23, 2008

Sudoxicam and meloxicam are nonsteroidal anti-inflammatory drugs (NSAIDs) from the enol-carboxamide class. While the only structural difference between the two NSAIDs is the presence of a methyl group on the C5-position of the 2-carboxamidothiazole motif in meloxicam, a marked difference in their toxicological profile in humans has been discerned. In clinical trials, sudoxicam was associated with several cases of severe hepatotoxicity that led to its discontinuation, while meloxicam has been in the market for over a decade and is devoid of hepatotoxicity. In an attempt to understand the biochemical basis for the differences in safety profile, an *in vitro* investigation of the metabolic pathways and covalent binding of the two NSAIDs was conducted in NADPH-supplemented human liver microsomes. Both compounds demonstrated NADPH-dependent covalent binding to human liver microsomes; however, the extent of binding of [^{14}C]-meloxicam was ~2-fold greater than that of [^{14}C]-sudoxicam. While inclusion of glutathione (GSH) in microsomal incubations resulted in a decrease in covalent binding for both NSAIDs, the reduction in binding was more pronounced for meloxicam. Metabolite identification studies on [^{14}C]-sudoxicam in NADPH-supplemented human liver microsomes indicated that the primary route of metabolism involved a P450-mediated thiazole ring scission to the corresponding acylthiourea metabolite (S3), a well-established pro-toxin. The mechanism of formation of S3 presumably proceeds via (a) epoxidation of the C4−C5-thiazole ring double bond, (b) epoxide hydrolysis to the corresponding thiazole-4,5-dihydrodiol derivative, which was observed as a stable metabolite (S2), (c) ring opening of the thiazole-4,5-dihydrodiol to an 2-oxoethylidene thiourea intermediate, and (d) hydrolysis of the imine bond within this intermediate to yield S3. In the case of meloxicam, the corresponding acylthiourea metabolite M3 was also observed, but to a lesser extent; the main route of meloxicam metabolism involved hydroxylation of the 5′-methyl group, a finding that is consistent with the known metabolic fate of this NSAID. Inclusion of GSH led to a decrease in the formation of M3 with the concomitant formation of an unusual two-electron reduction product (metabolite M7). The formation of M7 is proposed to arise via reduction of the imine bond in 2-oxopropylidene thiourea, an intermediate in the thiazole ring scission pathway in meloxicam. In conclusion, the results of our analysis suggest that if the covalent binding of the two NSAIDs is important to the overall hepatotoxicity risk, the differences in metabolism (differential preponderance of formation of the acylthiourea relative to total metabolism), differential effects of GSH on covalent binding, and finally differences in daily doses of the two NSAIDs may serve as a plausible explanation for the marked differences in toxicity.

Introduction

Enol-carboxamides are a well-established class of nonsteroidal anti-inflammatory drugs (NSAIDs[1]) with several marketed representatives including piroxicam, tenoxicam, lornoxicam and meloxicam (Figure 1). The biochemical basis for anti-inflammatory action of enol-carboxamides involves reversible inhibition of cyclooxygenase (COX) enzymes in a fashion similar to that discerned with the classical carboxylic acid-containing NSAIDs (e.g., indomethacin and ibuprofen) (*1*). A common structural feature in the enol-carboxamide class of NSAIDs is the presence of the 4-hydroxy-2-methyl-2*H*-1,2-arylthiazine-3-carboxamide 1,1-dioxide motif. Mechanistic studies designed to explore the molecular basis of COX inhibition by enol-carboxamides suggest that the weakly acidic keto−enol group (p*K*a ~5.2) at position C4 functions as a carboxylic acid bioisostere and inhibits COX activity by binding to active site amino acid residue(s) identical to the ones bound by classical carboxylate-containing NSAIDs (*2*).

While the 4-hydroxy-2-methyl-2*H*-1,2-arylthiazine-3-carboxamide 1,1-dioxide scaffold has been extensively exploited toward the discovery of new anti-inflammatory drugs, cases of failure also exist. Sudoxicam (4-hydroxy-2-methyl-*N*-(2-thiazolyl)-2*H*-1,2-benzothiazine-3-carboxamide-1,1-dioxide, Figure 1) was the first enol-carboxamide reported to have efficacy in various animal models of inflammation (*3, 4*). While the compound demonstrated anti-inflammatory action in extensive clinical trials, its clinical development was discontinued due to incidences of severe hepatotoxicity (*5*). Interestingly, the clinical

* To whom correspondence should be addressed. Tel: (860)-441-6122. E-mail: r.scott.obach@pfizer.com.

[1] Abbreviations: NSAIDs, nonsteroidal anti-inflammatory drugs; COX, cyclooxygenase; sudoxicam, 4-hydroxy-2-methyl-*N*-(2-thiazolyl)-2*H*-1,2-benzothiazine-3-carboxamide-1,1-dioxide; meloxicam, 4-hydroxy-2-methyl-*N*-(5-methyl-2-thiazolyl)-2*H*-1,2-benzothiazine-3-carboxamide-1,1-dioxide; DILI, drug-induced liver injury; LC-MS/MS, liquid chromatography mass spectrometry; CID, collision-induced dissociation.

10.1021/tx800185b CCC: $40.75 © 2008 American Chemical Society
Published on Web 08/16/2008

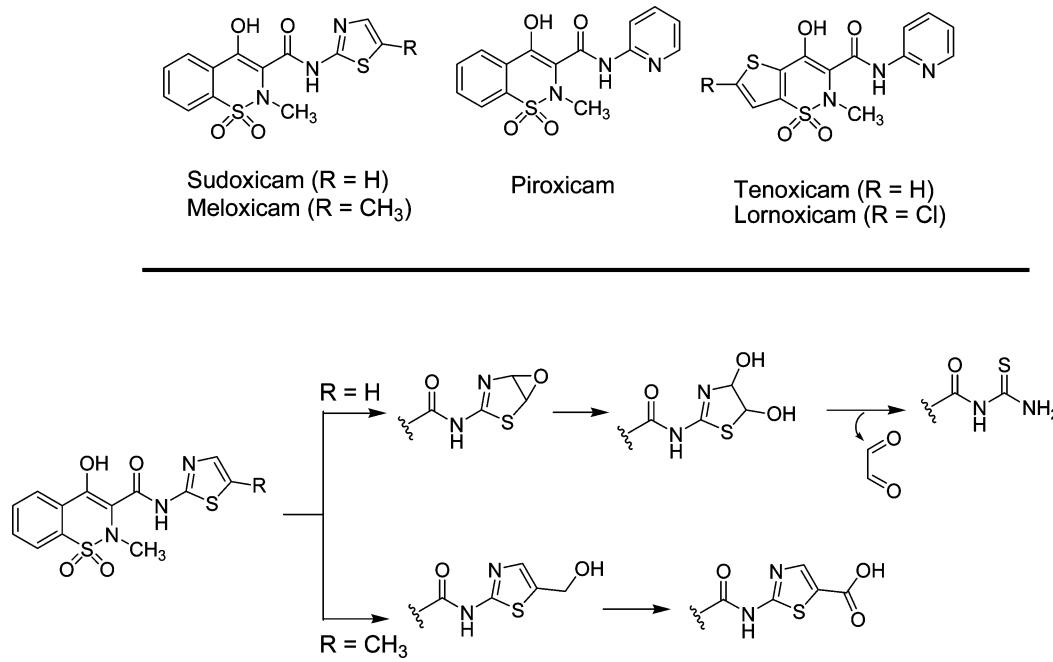

Figure 1. Structures of enol-carboxamide class of NSAIDs.

observations on sudoxicam hepatotoxicity are in stark contrast to the vastly superior safety profile of the closely related analog meloxicam (4-hydroxy-2-methyl-*N*-(5-methyl-2-thiazolyl)-2*H*-1,2-benzothiazine-3-carboxamide-1,1-dioxide, Figure 1), which is commonly prescribed as an anti-inflammatory agent in humans and veterinary applications. Since its introduction in 1995, reports of drug-induced liver injury (DILI) associated with meloxicam have been extremely rare (*6*).

In many cases, an in-depth understanding of the molecular basis for toxicity has been useful in replacing a vague perception of a chemical class effect with a sharper picture of an individual chemical peculiarity. With sudoxicam and meloxicam, the only structural difference is the presence of a methyl group on the 5-position of the thiazole ring in meloxicam (Figure 1). However, the minor change in structure dramatically alters the metabolic profile of the two drugs. Early studies on the metabolism of sudoxicam in animals indicated the exclusive formation of acylthiourea metabolite(s) obtained from thiazole ring scission (Figure 1) (*7*). Fairly strong evidence linking thiazole ring bioactivation to subsequent hepatotoxic response in preclinical species and/or humans has been presented with numerous thiazole-containing xenobiotics including drugs (*8*−*11*). Following enzymatic thiazole ring scission, acylthioureas are susceptible to further *S*-oxidation to electrophilic sulfenic and sulfinic acid derivatives capable of oxidizing critical biomacromolecules or depleting glutathione (GSH) (*8, 9, 12*). A similar mechanism of *S*-oxidation has also been proposed to account for the hepatotoxicity associated with thiobenzamides (*13*). On the basis of these studies, it is possible that reactive metabolites derived from thiazole ring opening in sudoxicam play a causal role in the clinical hepatotoxicity. Additional evidence supporting this proposal stems from the findings on meloxicam metabolism in humans, which presumably does not involve thiazole ring scission; instead, oxidation of the C-5 thiazole methyl group to an alcohol and carboxylic acid derivative (Figure 1) is the principal metabolic fate of this NSAID in humans (*14*). While this hypothesis sounds logical there is no experimental evidence to support it; all evidence is thus far circumstantial. Consequently, we decided to conduct a side-by-side comparison of the in vitro bioactivation and covalent binding potential of [^{14}C]-sudoxicam and [^{14}C]-meloxicam in human liver microsomes. The findings are described herein.

Experimental Procedures

Chemicals. [^{14}C]-Sudoxicam and [^{14}C]-meloxicam were obtained from Nerviano Medical Sciences (Milan, Italy) and were of >98% radiopurity. Materials were repurified by HPLC prior to incubations. The site of radiolabel was the carbonyl carbon. Sudoxicam was obtained from the sample bank at Pfizer, while meloxicam, GSH, and β-NADPH were purchased from Sigma-Aldrich (St. Louis, MO). Pooled human liver microsomes were prepared under contract by BD Gentest (Woburn, MA). $H_2{}^{18}O$ was obtained from Cambridge Isotope Laboratories (Woburn, MA) and ^2H_2O was from Isotec (Miamisburg, OH).

Microsomal Incubations. [^{14}C]-Sudoxicam or [^{14}C]-meloxicam (54 mCi/mmol) mixed with unlabeled drugs, at 50 μM were incubated with human liver microsomes (2.0 mg/mL) in 100 mM potassium phosphate buffer (pH 7.4) containing $MgCl_2$ (3.3 mM) and NADPH (1.3 mM). In cases where GSH was used, its concentration was 5 mM. Incubations were commenced with the addition of microsomes, and were conducted in a shaking water bath maintained at 37 °C open to the air. After 1 h, the incubations were terminated by addition of five volumes of acetonitrile, mixed vigorously, and the precipitated materials were removed by spinning in a centrifuge (1700*g*) for 5 min. The supernatants were transferred to a clean tube and evaporated in a vacuum centrifuge. The residues were reconstituted in 0.2 mL aqueous formic acid (0.1%) for analysis by liquid chromatography ion trap mass spectrometry (LC-MS/MS).

Biosynthesis of Metabolites. In general, metabolite biosynthesis was done using the following approach. In a total volume of 2 mL was included sudoxicam or meloxicam (50 μM), liver microsomes (4 mg/mL), $MgCl_2$ (3.3 mM), and NADPH (1.3 mM) in potassium phosphate buffer (0.1 M, pH 7.4). Incubations were carried out for 1 h at 37 °C after which they were terminated by addition of 0.5 mL HCl (1M). For the preparation of meloxicam metabolite M7, GSH was included at 5 mM. For the preparation of metabolite S2 and S3, liver microsomes from phenobarbital-induced male rats were used to increase the respective yields. Terminated incubation mixtures were extracted with methyl-*tert*-butyl ether (2 × 4 mL), and the extracts were combined and dried under N_2. The residues were reconstituted in 0.1 mL 0.1% formic acid containing 20% acetonitrile and injected onto the HPLC using the conditions

described below. The effluent was collected into 20 s fractions, and fractions containing the desired products, as assessed by MS, were combined for further characterization.

A biosynthesis of M7 was carried out on a larger scale to generate enough material for ^{1}H NMR analysis. The incubation was conducted as above in a 50 mL volume. After acidification (10 mL HCl, 1 M), the mixture was extracted with methyl-*tert*-butyl ether (2 × 60 mL), the organic fraction was evaporated and the residue was reconstituted in 0.1% formic acid containing 5% acetonitrile. The reconstituted mixture was spun in a centrifuge for 20 min at 17000*g* and the supernatant was applied to a Polaris C18 column (4.6 × 250 mm; 5 μm Varian, Lake Forest, CA) at 0.8 mL/min using a Jasco HPLC pump. After the material was applied to the column, M7 was eluted using the mobile phase gradient described below. Fractions were collected every 20 s, and the fractions containing M7 were pooled, evaporated under vacuum, reconstituted in 0.2 mL mobile phase and repurified on HPLC. The fractions containing pure M7 were pooled and evaporated under vacuum for ^{1}H NMR characterization.

Chemical/Metabolic Studies with S3 and M7 Metabolites. To better understand the metabolism of sudoxicam and meloxicam, some of the isolated metabolites were subjected to further chemical analysis. Metabolites S3 and M7 were subjected to an overnight incubation under acidic and alkaline conditions. Fractions containing these metabolites were acidified to pH ~1 with trifluoroacetic acid and alkalinized to pH ~10 with ammonium hydroxide, allowed to stand overnight at ambient temperature and analyzed by LC-MS/MS. For S3, the acidic incubation was also carried out in 50% $H_2{}^{18}O$. Metabolite S3 (1.2 μM) was subjected to further metabolism in the presence of human liver microsomes (2 mg/mL), $MgCl_2$ (3.3 mM), NADPH (1.3 mM) in 0.2 mL phosphate buffer (0.1 M, pH 7.4) for 30 min at 37 °C in the presence and absence of GSH (5 mM). Incubations were terminated with the addition of acetonitrile, processed as described above, and analyzed by LC-MS/MS. Metabolite M7 was subjected to treatment with 2 mg NaB^2H_4 for 30 min followed by acidification and analysis by LC-MS/MS.

LC-MS/MS Analysis. The LC system consisted of a Finnigan Surveyor HPLC injector, quaternary pump and diode array detector in line with an LTQ ion trap mass spectrometer and Gilson fraction collector. The column used was a Polaris C18 (4.6 × 250 mm; 5 μm) at a flow rate of 0.8 mL/min. The mobile phase consisted of 0.1% formic acid (A) and acetonitrile (B). The gradient consisted of 5% B for 5 min followed by a linear gradient to 30% B at 10 min, 55% B at 40 min, and 95% B at 45 min. This was followed by a 10 min reequilibration of the column at 95% B. The effluent was passed through the diode array detector operated in the wavelength range of λ 200 to 400 nm. This was followed by introduction, at a split of approximately 20 to 1, into the source of the LTQ mass spectrometer operated in the negative ion mode (source potential, 4 kV; capillary potential, −12V; source temperature, 350 °C), with data dependent scanning to MS^3 of the top two ions by abundance (MS^2 and MS^3 normalized collision energies of 20 and 35, respectively). Fractions were collected every 20 s into Wallac Scintiplates. The LC eluent was evaporated in a Genevac vacuum centrifuge and analyzed on a Wallac Microbeta scintillation counter (Wallac; Turku, Finland). In some cases, fractions containing metabolites were isolated and infused into a Finnigan Orbitrap ion trap mass spectrometer using similar tuning parameters to obtain high resolution spectral data.

NMR Analysis. All NMR spectra were recorded on a Bruker Avance 600 MHz (Bruker BioSpin Corporation, Billerica, MA) controlled by TOPSPIN V2.0 and equipped with a 2.5 mm BBI probe. 1D spectra were recorded using a sweep width of 11000 Hz and a total recycle time of 5 s. The resulting time-averaged free induction decays were transformed using an exponential line broadening of 0.3 Hz to enhance signal-to-noise.

Covalent Binding Determination. To measure the extent of metabolism-dependent covalent binding of [^{14}C]-sudoxicam and [^{14}C]-meloxicam in microsomes, incubations were conducted in a manner similar to that described above. Incubations were terminated with five volumes of acetonitrile, vigorously mixed, and spun in a centrifuge at 1700*g* for 5 min. The supernatant was discarded, the pellet suspended in 1 mL water, 5 mL acetonitrile and 1 mL methanol was added, the sample was mixed and spun in a centrifuge as before. The pellet was subjected to this treatment three more times using water and acetonitrile. After the fifth wash, the pellet was washed three more times with just acetonitrile. No radioactivity above background readings was detected in the washing solvent of the final two washes. The pellets were dissolved in 1 mL NaOH (2N) overnight, followed by addition of 1 mL water and 18 mL TruCount scintillation fluid for determination of radioactivity. The radioactivity in the incubated samples was compared to residual radioactivity in samples prepared in an identical fashion but not incubated. Calculations were done based on the nominal protein concentration in the incubation.

Table 1. Metabolism-Dependent Covalent Incorporation of [^{14}C]-Sudoxicam and [^{14}C]-Meloxicam into Human Liver Microsomal Protein

	sudoxicam	meloxicam
Covalent Incorporation (pmol bound/mg protein)[a]		
−GSH	1.4 ± 0.1	3.6 ± 0.2
+GSH (5 mM)	0.74 ± 0.06	0.28 ± 0.02

[a] Calculation of covalent binding was based on the nominal protein concentration in the incubation.

Results

Covalent Binding in Human Liver Microsomes. The results from covalent binding studies following incubations of [^{14}C]-sudoxicam and [^{14}C]-meloxicam with NADPH-supplemented human liver microsomes are listed in Table 1. Addition of GSH to microsomal incubations caused a marked decrease in covalent incorporation of radioactivity. In liver microsomes, meloxicam showed a greater amount of covalent incorporation than sudoxicam, but with addition of GSH, the order was reversed. Only about half of the covalent incorporation of sudoxicam was blocked by addition of GSH.

Metabolism of Sudoxicam and Meloxicam in Human Liver Microsomes. In order to gain an insight into the structure of the reactive species responsible for covalent binding, the metabolism of the two NSAIDs was characterized in human liver microsomes. In human liver microsomal incubations, between 3.2 to 4.5% of sudoxicam and meloxicam were consumed with three metabolites of sudoxicam (denoted S2, S3, and S4) and six metabolites of meloxicam (denoted M2-M7) observed (Figure 2). The formation of these metabolites was NADPH-dependent. In the presence of GSH, S4 was not observed as a metabolite of sudoxicam. In meloxicam incubations, metabolite M7 was only observed in the presence of GSH, and M4 was not observed. Collision-induced dissociation (CID) mass spectra for sudoxicam, meloxicam, and their respective metabolites in negative ion mode are depicted in Figures 3 and 4. The fragmentation pattern for sudoxicam was fairly simple to interpret (see CID spectrum in Figure 3), with major ions present at *m*/*z* 272 (loss of 64 mass units; i.e., SO_2), *m*/*z* 210 representing the anion of *N*-methyl-1,2-benzothiazin-4-ol 1,1-dioxide, and *m*/*z* 146 (loss of SO_2 from *m*/*z* 210). For meloxicam, the fragmentation pattern (see CID spectrum in Figure 4) is identical to that observed for sudoxicam (i.e., loss of SO_2 at *m*/*z* 286, generation of the anion of *N*-methyl-1,2-benzothiazin-4-ol 1,1-dioxide at *m*/*z* 210, and loss of SO_2 from the latter ion to form *m*/*z* 146). These interpretations were corroborated by high resolution spectral data, and all *m*/*z* values were 5.5 ppm from theoretical, or less.

Sudoxicam Metabolite S2. S2 possessed a molecular ion (M-1) of *m*/*z* 370, an addition of 34 mass units indicating an

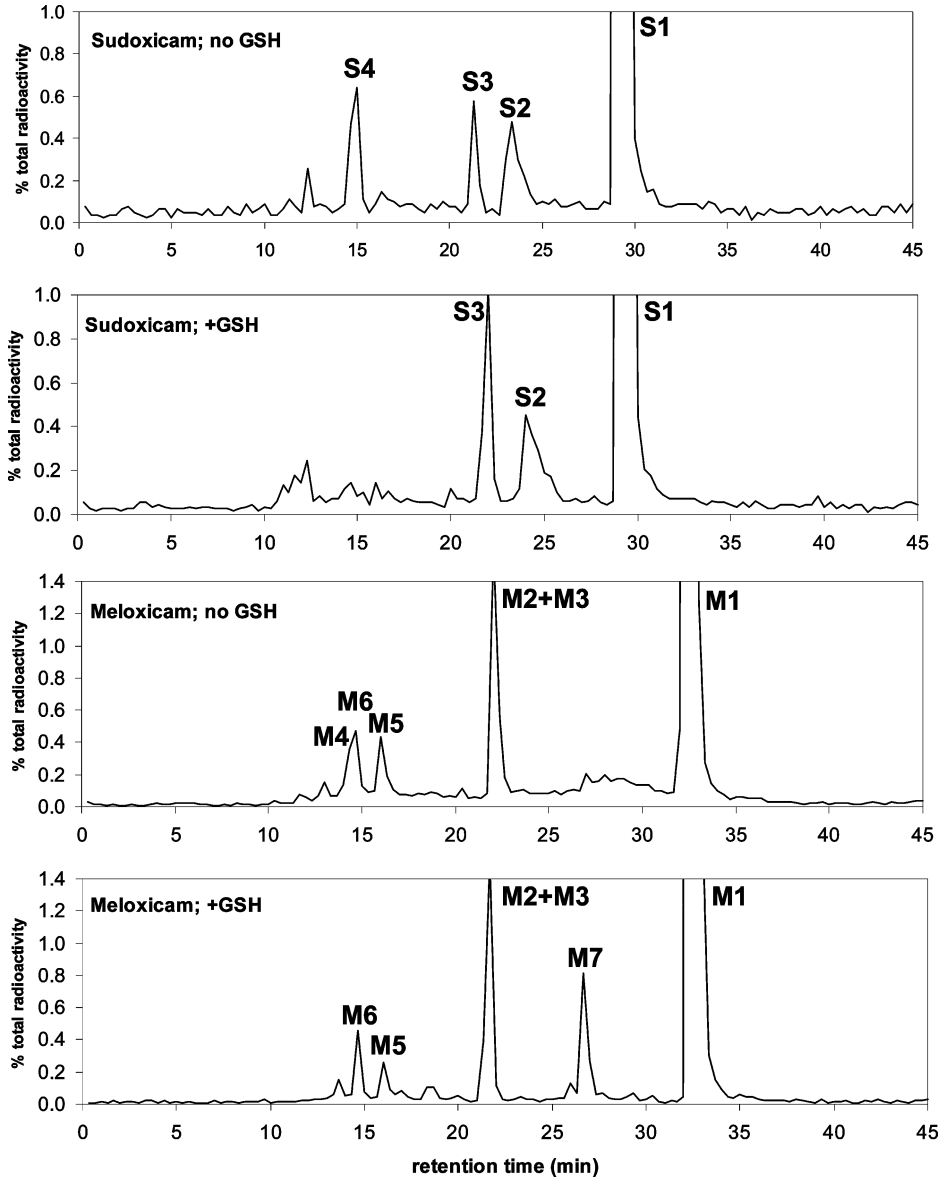

Figure 2. Radiometric chromatograms of NADPH-supplemented human liver microsomal incubation mixtures of sudoxicam and meloxicam. Key: S1 = unchanged sudoxicam; S2 = sudoxicam dihydrodiol; S3 = thiourea metabolite; S4 = oxidized thiourea metabolite; M1 = unchanged meloxicam; M2 = 5′-hydroxymeloxicam; M3 = thiourea metabolite; M4 = oxidized thiourea metabolite; M5 = cyclized metabolite; M6 = oxidized meloxicam metabolite; M7 = reduced open-ringed meloxicam metabolite.

oxidation and addition of water. The proposed structure of this metabolite is shown in Figure 3. Metabolite S2 comprised about half of the metabolism of sudoxicam. The pathway leading to the formation of S2 most likely involves P450-mediated oxidation of the thiazole 4,5-double bond to afford the unstable epoxide intermediate; spontaneous hydrolysis of which, affords the thiazole-4,5-dihydrodiol metabolite S2. As shown in Figure 3 (CID spectrum of S2), the fragment ion at *m/z* 253, proposed as the *N*-methyl-1,2-benzothiazin-3-carboxyamide-4-ol 1,1-dioxide anion strongly suggests the thiazole ring as the site of modification. Further fragmentation of *m/z* 253 yields *m/z* 210 (loss of O═C═NH) and *m/z* 189 (loss of SO_2), consistent with the assignment. The fragment ion at *m/z* 202 is consistent with a proposed structure of H_3C-N═C^--C(═O)-NH-(2-(4,5-dihydoxythiazole), and this fragment subsequently yields *m/z* 171 (loss of methylamine) and *m/z* 116 (4,5-dihydroxythiazole anion), consistent with the proposed structure shown in Figure 3. In an incubation conducted in $H_2{}^{18}O$, the deprotonated molecular ion of *m/z* 372 was observed indicating that the source of one of the oxygen atoms was from water, consistent with a mechanism involving initial thiazole ring epoxidation followed by hydrolysis. Fragment ions from *m/z* 372 (the ^{18}O-containing metabolite) yielded *m/z* 253, 204, and 189 (Figure 5); ions 253 and 189 associated with the *N*-methyl-1,2-benzothiazin-3-carboxyamide-4-ol 1,1-dioxide portion did not contain ^{18}O while *m/z* 204 contained ^{18}O showing that the water-derived oxygen atom resides on the thiazole portion, and consistent with the assigned structure. Specific searching for a GSH adduct of the proposed epoxide intermediate did not yield any signal in the total ion current, and the approximate amount of S2 formed did not appear to decrease with inclusion of GSH.

Sudoxicam Metabolite S3. Metabolite S3 had a deprotonated molecular ion at *m/z* 312 (Figure 3), consistent with the acylthiourea metabolite derived from thiazole ring scission. The *in vivo* formation of S3 has been described previously by Hobbs and Twomey (*7*) following oral or intravenous administration of [^{14}C]-sudoxicam to animal species. An exact mass of 312.00905 (−5.4 ppm) was obtained for this metabolite, consistent with the assigned structure. Fragment ions of *m/z* 253 (loss of HSCN; *m/z* 253.02775; −0.02 ppm), *m/z* 248 (loss of

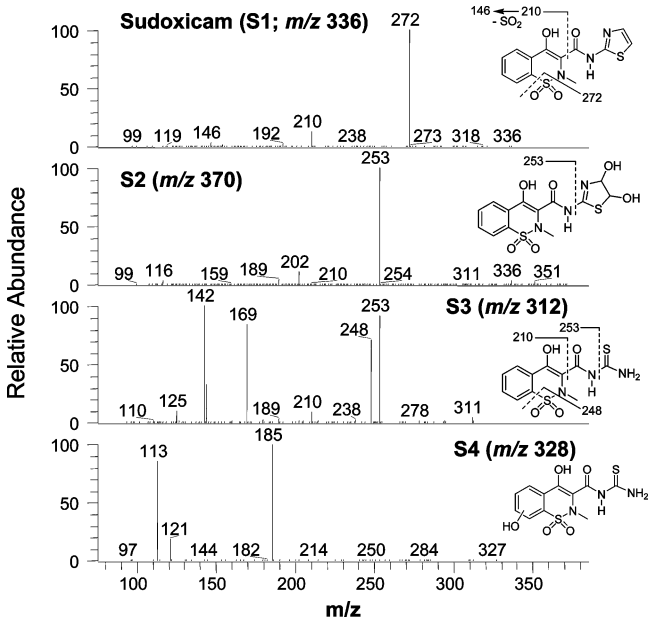

Figure 3. CID spectra of sudoxicam and S2, S3, and S4 metabolites.

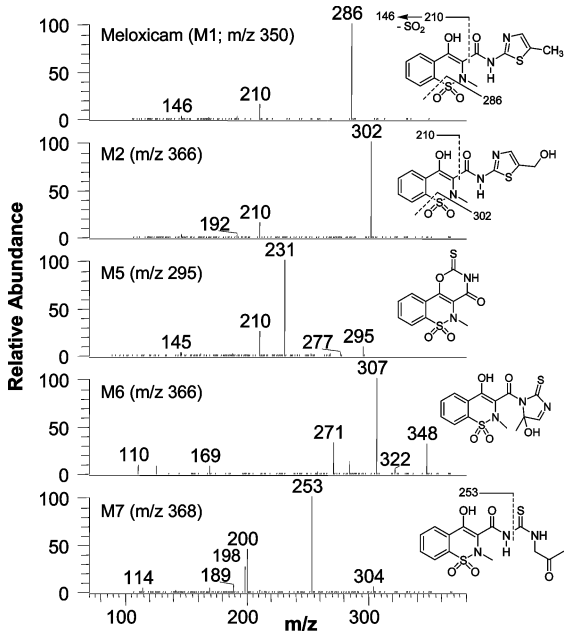

Figure 4. CID spectra of meloxicam and M2, M5, M6, and M7 metabolites.

SO_2), *m/z* 210 (anion of *N*-methyl-1,2-benzothiazin-4-ol 1,1-dioxide), *m/z* 169 (2-hydroxy-1,1-dioxybenzothietane anion; 168.99596; 3.3 ppm), and *m/z* 142 (proposed as a cyclized fragment; the anion of 4-methyliminoimidazoline-2-thione-5-one from high resolution mass spectral data; *m/z* 142.00765; 5.1 ppm) were observed and are consistent with the proposed structure. Further fragmentation of the *m/z* 253 ion in the ion trap yielded *m/z* 189 (loss of SO_2) and *m/z* 210 (loss of *O*=C=NH). Incubation of S3 (isolated from microsomal incubations) in weakly alkaline conditions gave rise to M5, a metabolite observed in liver microsomal incubations with meloxicam (see below), whereas incubation of S3 in acidic conditions or in NADPH-supplemented liver microsomes yielded S4 (see below). In the absence of GSH, S3 comprised about a quarter of the metabolism of sudoxicam, while that increased to about half-in the presence of GSH, presumably due to the absence of metabolite S4 when GSH was included (see below).

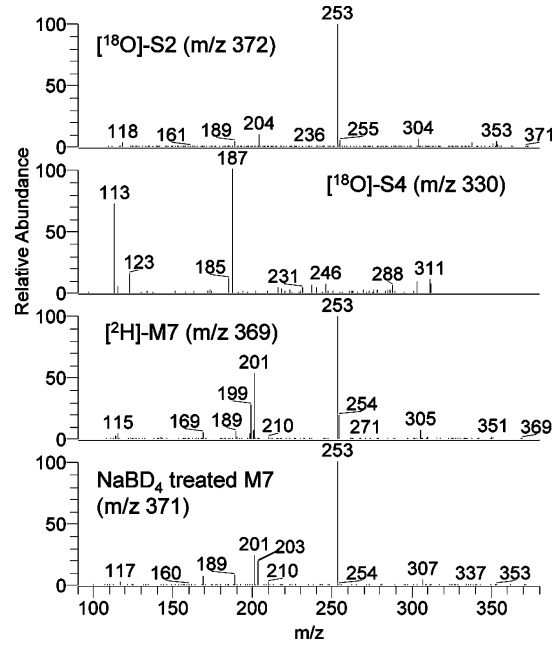

Figure 5. CID spectra for metabolite S2 containing ^{18}O (*m/z* 372), S4/M4 generated from S3/M3 in acid and containing ^{18}O (*m/z* 330), M7 containing deuterium (*m/z* 369; generated in deuterated water), and M7 after reduction with $NaBD_4$ (*m/z* 371).

Sudoxicam Metabolite S4. Metabolite S4 had a deprotonated molecular ion of *m/z* 328, consistent with monohydroxylation of S3. The fragment ion at *m/z* 185 is analogous to *m/z* 169 observed as a fragment ion of S3 with additional 16 Da, suggesting that the position of hydroxylation is on the phenyl ring (Figure 3). Further fragmentation of *m/z* 185 yielded *m/z* 121 indicating loss of SO_2. Interestingly, inclusion of GSH in the microsomal incubations led to a complete disappearance of S4 with a concomitant increase in the peak of the thiourea metabolite S3 (see Figure 2). The hypothesis that S4 is derived from metabolism of S3 was explored after biosynthesis and isolation of S3 followed by incubation in NADPH-supplemented human liver microsomes (Figure 6). In the absence of GSH, NADPH-supplemented human liver microsomal incubations of S3 led to the formation of S4; the amount of S4 formed was completely abolished in the presence of GSH. Finally, a small amount of S4 was also formed from S3 in incubations in acidic buffer. When the incubation was done in 50% $H_2{}^{18}O$, the molecular ion for S4 increased by 2 Da to *m/z* 330, indicating that the origin of the oxygen atom was derived from water. Daughter ions for *m/z* 330 included *m/z* 187 and 123 instead of *m/z* 185 and 121, consistent with the addition of the oxygen on the phenyl ring. A proposed structure for S4 which is consistent with the CID spectrum is shown in Figure 3. A mechanism for formation of S4 is not readily apparent and merits further investigation.

Meloxicam Metabolite M2. The major metabolite of meloxicam, designated as peak M2, arises by the addition of 16 Da to parent drug and yields a fragmentation pattern consistent with monohydroxylation occurring on the 5-methylthiazole portion of meloxicam (see CID spectrum of M2 in Figure 4). M2 comprised about half of the metabolism of meloxicam, assessed by radioactivity (Figure 2). By analogy to previously reported work, the structure of M2 is proposed as the 5-hydroxymethylthiazolyl metabolite of meloxicam (*15, 16*). Structural assignment based on mass spectral data was further corroborated by ^1H NMR data (Table 2), which is consistent with the previously reported ^1H NMR spectrum of this metabolite (*15*).

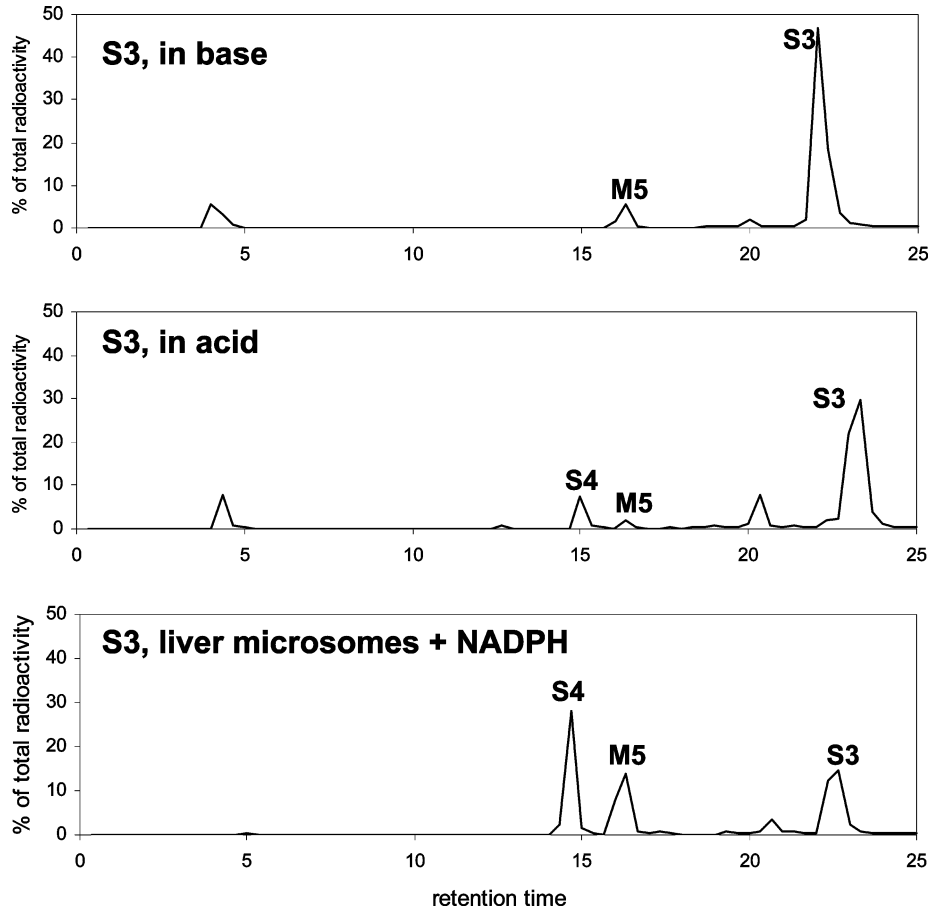

Figure 6. Radiometric chromatograms of S3 incubated with acid, base, and in a liver microsomal incubation.

Table 2. H NMR Chemical Shifts (ppm) for Meloxicam, M2, and M7

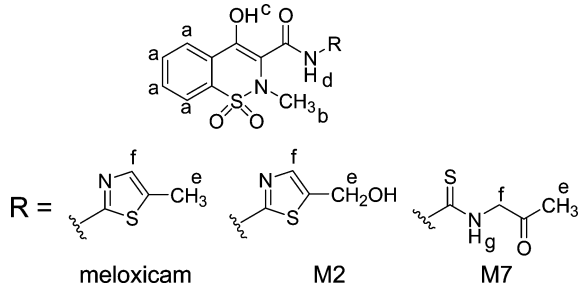

protons	meloxicam	M2	M7
ArH (a)	8.02 (d, J = 7.8 Hz, 1H)	7.89 (d, J = 8.3 Hz, 1H)	8.01 (d, J = 7.8 Hz, 1H)
	7.71 (m, 1H)	7.45 (d, J = 7.8 Hz, 1H)	7.73 (m, 1H)
	7.61 (m, 2H)	7.16 (m, 1H)	7.64 (m, 2H)
		7.14 (m, 1H)	
b	2.74 (s, 3H)	2.75 (s, 3H)	2.73 (s, 3H)
c	12.78 (s, 1H)	11.8 (s, 1H)	not observed
d	14.38 (s, 1H)	14.5 (s, 1H)	13.86 (s, 1H)
e	2.31 (d, J = 1.3 Hz, 3H)	4.54 (d, J = 5.8 Hz, 2H)	2.16 (s, 3H)
f	6.99 (d, J = 1.3 Hz, 1H)	7.14 (s, 1H)	4.47 (d, J = 4.8 Hz, 2H)
g			11.44 (t, J = 4.8 Hz, 1H)

Meloxicam Metabolite M3. Metabolite M3 coeluted with M2 but was present in considerably lower abundance. The CID spectrum of M3 was identical to the sudoxicam metabolite S3 and represents the acylthiourea metabolite that arises via thiazole ring scission in meloxicam. Using the peak response for S3 as a calibrant, it was estimated that M3 comprised 3−4% of total metabolism of meloxicam. The formation of M3 was slower than the formation of S3 from sudoxicam and comprised a much lower fraction of total metabolism.

Meloxicam Metabolite M4. The metabolite designated as M4 in the meloxicam incubation HPLC trace is identical to sudoxicam metabolite S4, possessing a deprotonated molecular ion at *m*/*z* 328, 16 Da greater than M3. In the LC radiometric trace, M4 eluted as a front shoulder to the M6 peak. As with sudoxicam metabolite S4, meloxicam metabolite M4 was not observed when GSH was included in the incubation.

Meloxicam Metabolite M5. Meloxicam metabolite M5 had a deprotonated molecular ion of *m*/*z* 295 which was consistent with the 2-thioxo-2,3-dihydro-1,3-oxazin-4-one derivative shown in Figure 4. Diagnostic fragments in the CID spectrum of M5 included fragment ions at *m*/*z* 231 (loss of SO_2; 64 mass units) and at *m*/*z* 210 (described as above for parent drug). Cyclization

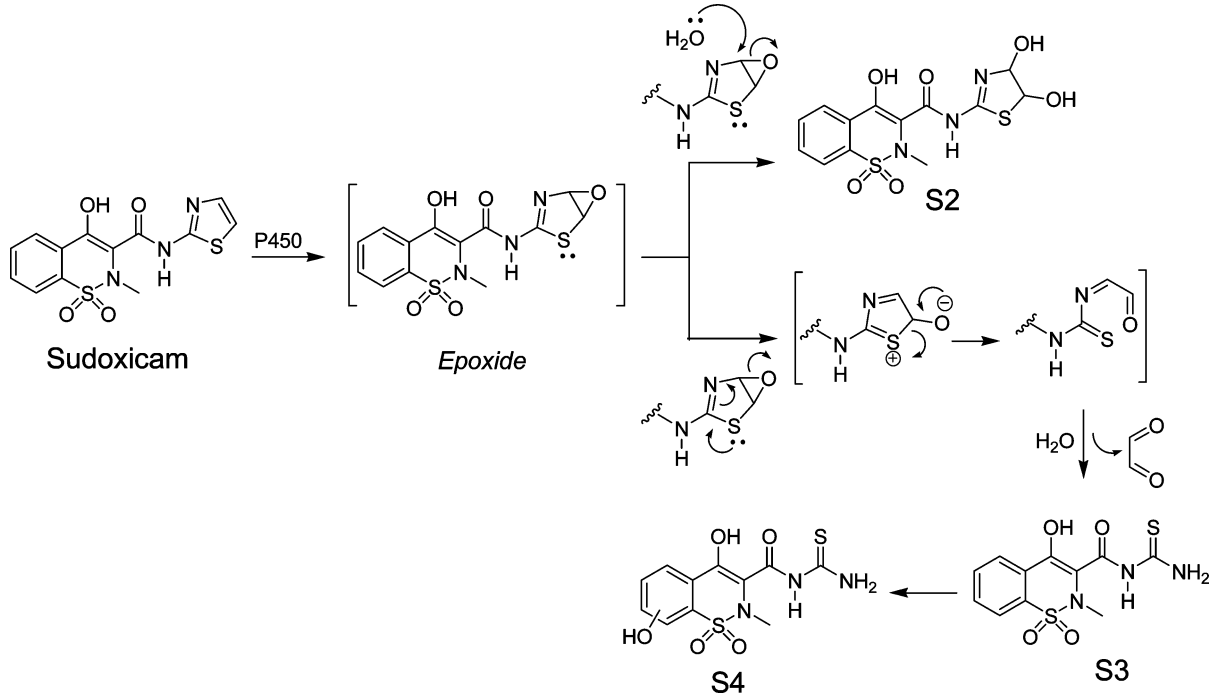

Figure 7. Proposed metabolic pathways for sudoxicam in human liver microsomes.

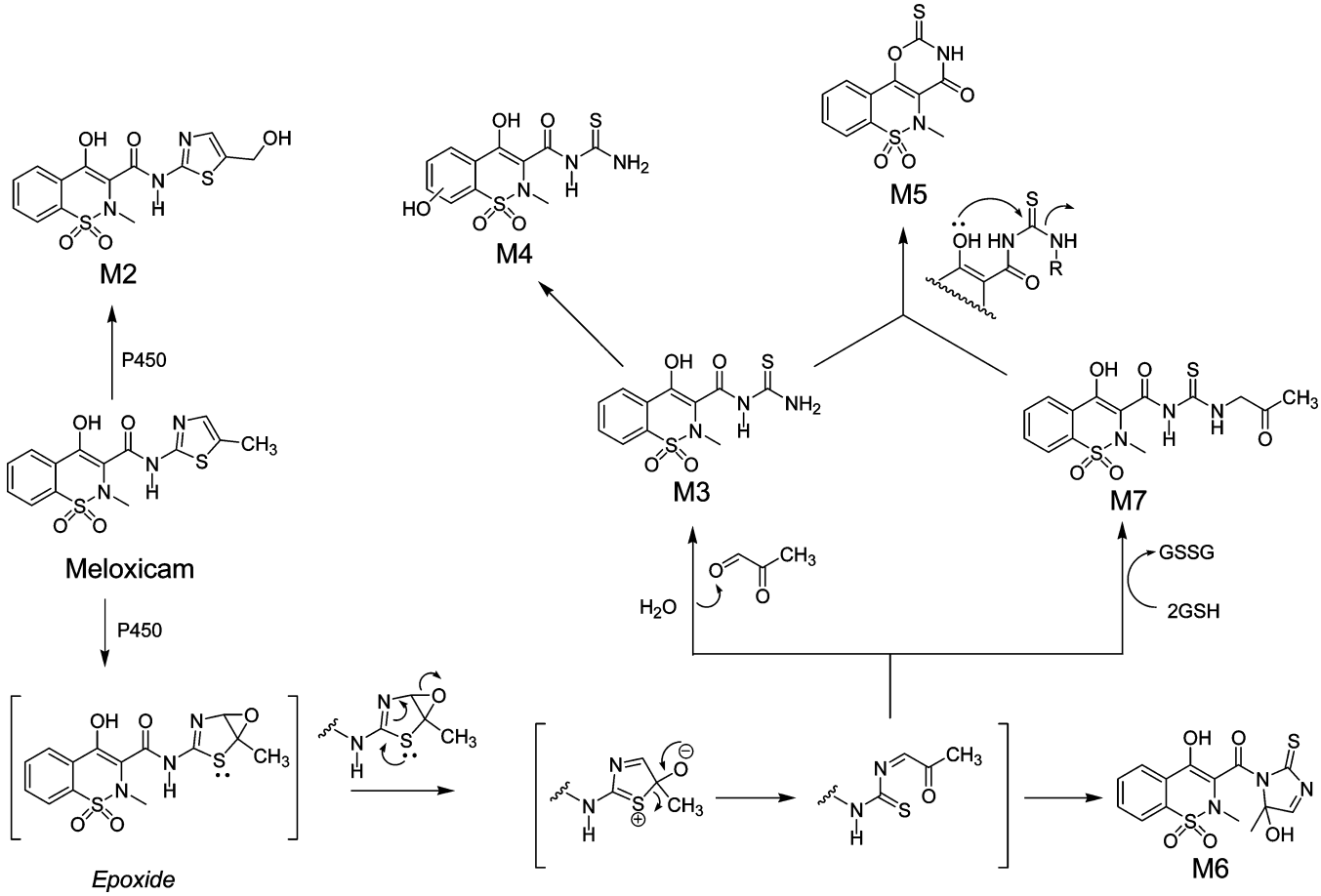

Figure 8. Proposed metabolic pathways for meloxicam in human liver microsomes.

of acylthiourea metabolite(s) of meloxicam to afford corresponding pyrimidine-dione metabolites has been described before in the rat (*15*). In the present case, the proposed mechanism of formation of M5 is shown in Figure 8 and involves initial nucleophilic attack by the enolic OH group on the thiocarbonyl group in a meloxicam acylthiourea metabolite(s) followed by spontaneous elimination of the amine (ammonia for M3; 1-amino-2-propanone for M7). Metabolite M5 was also observed when acylthiourea metabolites, M3 and M7, were isolated and allowed to stand overnight under weakly alkaline conditions (pH ~10) but not under acidic conditions (pH ~1).

Meloxicam Metabolite M6. Metabolite M6 had a deprotonated molecular ion of *m/z* 366, 16 Da greater than the parent compound and consistent with the addition of an oxygen atom. Major fragment ions were *m/z* 348, 307, and 271 (see Figure 4). Exact mass data for *m/z* 307 yielded a value of 307.0387 consistent with a loss of HSCN and suggesting that thiazole ring scission followed by a rearrangement had to occur to accommodate this loss. The fragment ion at *m/z* 348 suggests loss of water and subsequent fragmentation of *m/z* 348 yielded *m/z* 284, a loss of 64 mass units (SO_2). Further fragmentation of *m/z* 307 yielded *m/z* 212, 199, and 110 as fragment ions. While a detailed characterization of this metabolite was not performed, a structure that appears to be consistent with the observed CID spectrum is depicted in Figure 4. We speculate the formation of M6 to arise via intramolecular cyclization of the imino-carbonyl intermediate obtained via thiazole ring scission (see Figure 8). Additional characterization of this metabolite was not pursued.

Meloxicam Metabolite M7. Metabolite M7 was only observed when GSH was included in NADPH-supplemented human liver microsomes incubations of meloxicam. It had a deprotonated molecular ion of *m/z* 368, and an empirical formula of $C_{14}H_{14}O_5N_3S_2$ from high resolution mass spectral data (368.03468; −6.1 ppm). The fragment ion at *m/z* 253 (empirical formula of $C_{10}H_9O_4N_2S$ from exact mass data) is as described above for sudoxicam dihydrodiol and acylthiourea metabolites S2 and S3, respectively, and is consistent with modification on the 5-methylthiazole portion of the molecule. The unique fragment ion at *m/z* 200 is proposed as H_3C-N=C^--C(O)-NH-C(=S)-NH-CH_2-C(O)-CH_3 and the fragment at *m/z* 198 is analogous to the fragment ion at *m/z* 142 for sudoxicam metabolite S3; the additional 56 mass units are due to the acetonyl moiety. It is proposed that M7 arises from a GSH mediated reduction of an imine intermediate derived from the thiazole ring opening in meloxicam (see Figure 8). Incubations conducted in $H_2{}^{18}O$ or D_2O showed that the source of the oxygen atom was not from water (instead inferred to be from molecular oxygen) and that one of the hydrogens added was from water (or from a solvent exchanged proton on GSH). Fragmentation of the molecular ion possessing deuterium (*m/z* 369) still yielded *m/z* 253 showing that deuterium incorporation was not on the *N*-methyl-1,2-benzothiazin-4-ol-1,1-dioxide portion and fragment ions at *m/z* 201 and 199 were observed indicating that the deuterium was present on the acetonyl thiourea portion (Figure 5). Reduction of this metabolite with $NaBD_4$ yielded a compound with *m/z* 371 and fragment ions of *m/z* 253, 203, and 201 indicating that reduction occurred on the side chain, which is consistent with reduction of either a carbonyl or imine bond (Figure 5). Biosynthesis of M7 and analysis by NMR spectroscopy yielded a proton spectrum consistent with the assigned structure (Table 2). In the ^{1}H spectrum of the M7 metabolite, the hydrogen shifts of the *N*-methyl-1,2-benzothiazin-4-ol-1,1-dioxide portion of the molecule are present with only minor changes in chemical shift and coupling from that of similarly isolated meloxicam. The ^{1}H spectrum of M7 contains no resonance for the 4 position hydrogen of the meloxicam thiazole ring. Additionally, in the isolated metabolite, the C5-methyl protons shift upfield to 2.16 ppm and lose the weak coupling with the C4 thiazole ring hydrogen. Two new resonances, not observed in the meloxicam NMR spectrum, are present in the ^{1}H NMR spectrum of M7; a doublet at 4.47 ppm (J = 5.3 Hz, designated as protons f) integrating to two protons and a triplet at 11.44 ppm (J = 5.3 Hz, designated as proton g) integrating to a single proton (Table 2). These resonances are assigned as the methylene (4.47 ppm) and the adjacent thioamide (11.44 ppm) protons in the acetonyl thiourea motif in M7.

Discussion

Studies addressing the biochemical basis for the hepatotoxicity and/or renal toxicity of 2-amino- and/or 2-carboxamidothiazole-containing xenobiotics have provided strong evidence for the bioactivation of the thiazole ring system as a contributing factor in the underlying toxicities associated with these compounds (*8, 9*). In a manner similar to other 5-membered ring heterocycles such as thiophenes and furans (*10*), thiazole ring bioactivation involves oxidation on the C4−C5 ring double bond to generate an unstable epoxide; spontaneous hydrolysis of which leads to the corresponding dihydrodiol intermediate. Ring scission of the dihydrodiol then occurs, resulting in the liberation of glyoxal and the corresponding thiourea and/or acylthiourea as metabolites. Once formed, thiourea and acylthiourea metabolites can undergo *S*-oxidation to electrophilic sulfenic and/or sulfinic acid intermediates that can covalently modify or oxidize critical proteins leading to toxicity (*8, 9, 12*). A similar mechanism of toxicity has also been postulated for thiobenzamides (*13, 17*). Thus, it appeared reasonable to speculate that the idiosyncratic hepatotoxicity of sudoxicam in humans arose from metabolism of its thiazole ring to form reactive intermediates. The argument becomes even more compelling since meloxicam is not hepatotoxic, a feature which appears to be consistent with the lack of thiazole ring opening as a metabolic fate in humans.

However, to our surprise both sudoxicam and meloxicam demonstrated metabolism-dependent covalent binding to liver microsomes. The extent of microsomal covalent binding by the two NSAIDs even after incubation at 50 μM was much lower than that reported for prototypic hepatotoxins (typically >50 pmol/mg of protein at substrate concentrations of ∼ 10 μM). However, it is noteworthy to point out that covalent binding rates estimated in these studies need to be placed within context of total metabolism of the drug. If a drug is extensively but slowly metabolized then standard *in vitro* covalent binding experiments in liver microsomes may yield low levels of covalent binding. Consistent with the observed low clearance of 0.2 mL/min/kg (estimated hepatic extraction ratio of ∼1% based on human hepatic blood flow of 20 mL/min/kg) for meloxicam in humans (*14*), *in vitro* human liver microsomal incubations assessing metabolic stability of meloxicam and sudoxicam show very little depletion of these NSAIDs (*in vitro* $t_{1/2} \gg 60$ min). While the measured clearance of meloxicam in humans is very low, mass balance studies reveal extensive metabolism of this drug with only trace levels of parent NSAID detectable in urine and feces after 6 days (*14*). In contrast, even a small fraction of metabolism proceeding through a bioactivation pathway will yield higher rates for *in vitro* covalent binding for high clearance drugs prone to very rapid metabolism. This phenomenon was demonstrated in our recent studies on the side-by-side comparison of covalent binding by hepatotoxins and nonhepatotoxins (*18*).

In the absence of GSH, meloxicam exhibited greater binding in liver microsomes than sudoxicam, but the trend was reversed when GSH was included. The greater binding demonstrated by meloxicam when compared with sudoxicam probably reflects a subtle increase in the rate of P450-catalyzed metabolism of meloxicam. While the finding that GSH attenuates covalent binding to hepatic tissue is usually consistent with the scavenging of reactive metabolites by the sulfydryl nucleophile, in the

present case, no GSH conjugates derived from sudoxicam and/or meloxicam were observed in NADPH-supplemented liver microsomal incubations. For many thioureas that covalently bind to microsomes, addition of GSH abolishes covalent binding via reduction of the sulfenic acid metabolites and the concomitant formation of GSSG (*19*). Thus, GSH can be involved in the detoxication of thioureas as a cellular reductant for their reactive intermediates. It has been speculated that depletion of cellular GSH pools in mammals via continuous exposure of thiourea intermediates contributes to toxicity (*20*). The finding that the toxicity of 2-aminothiazoles is exacerbated in mice depleted of GSH by treatment with buthionine sulfoximine supports the protective role of the sulfydryl nucleophile against the toxicological response (*21, 22*). In the present study, two changes, however, were observed in the metabolic profile of meloxicam in human liver microsomes supplemented with NADPH and GSH. First, metabolite M4, which is derived from oxidation of the acylthiourea metabolite (M3) was no longer present and a new metabolite (M7) that is proposed to arise via a GSH-dependent reduction pathway was observed. For sudoxicam, the generation of metabolite S4 (the same as meloxicam metabolite M4) was also abolished when GSH was included in the microsomal incubations. The role of metabolites S4 and M4 as intermediates involved in the covalent binding of sudoxicam and meloxicam to liver microsomes is unknown at the present time. The likelihood that S4/M4 represent acylthiourea-*S*-oxides was not favored on the basis of mass spectral data. Since the effect of GSH on the binding of sudoxicam and meloxicam was different such that the effect on meloxicam was greater, the formation of M7 likely offsets covalent binding in some manner.

Proposed metabolic pathways of sudoxicam and meloxicam are shown in Figures 7 and 8. For sudoxicam (Figure 7), the rate-limiting step in its metabolism involved an initial P450-mediated epoxidation of the C4−C5 thiazole ring double bond. Hydrolysis of the epoxide yields the thiazole-4,5-dihydrodiol metabolite S2. In many cases, GSH is known to ring open epoxides, but no GSH adduct was observed in the radiometric trace, even upon specifically analyzing for the existence of such metabolite(s) in the total ion chromatograms (e.g., *m*/*z* 659). The epoxide ring opening can also be driven by the lone pair of electrons on the thiazole sulfur that would lead to the imino-aldehyde (see Figure 7), which upon imine bond hydrolysis yields acylthiourea S3. The acylthiourea metabolite can undergo further oxidation, either spontaneously or catalytically to form S4. S4 forms spontaneously under acidic conditions, and the formation in metabolic incubations, in which the oxygen is derived from water, is abolished by GSH. The exact structure of this metabolite is presently unknown and further work is ongoing to uncover the structure, understanding the mechanism for its formation, and any possible role for it in covalent binding. However, since the identical metabolite was also formed in microsomal incubations of meloxicam, it should not account for the underlying differences observed in covalent binding behavior and toxicological profile of the two NSAIDs.

While thiazole ring scission via initial epoxidation was also observed with meloxicam, it was apparently to a lesser extent, with M3 accounting for less than 5% of metabolism in microsomes. A key difference was the existence of an additional and major metabolic pathway P450-catalyzed hydroxylation on the 5-methylthiazolyl group leading to the 5′-hydroxymethylmeloxicam metabolite M2. M2 is known to undergo further oxidation to the corresponding carboxylic acid metabolite, a known end product of meloxicam metabolism *in vivo* (*14, 23*). This biotransformation sequence (methyl → primary alcohol → carboxylic acid) constitutes the major route of clearance of meloxicam *in vivo* in animals and humans accounting for >70% of meloxicam metabolism (*14, 23*) which may divert much of the dose of meloxicam away from reactive intermediates. Meloxicam epoxidation appears to follow the same rearrangement pathway to the acylthiourea, but in the presence of GSH reduction of the imine intermediate appears to occur, a difference from what was observed in the metabolism of sudoxicam. It is not presently known if this reduction is chemical or enzyme-catalyzed. While not reported in humans, ring opened acylthiourea metabolites of meloxicam similar to M7 have observed in rat *in vivo* (*15*). Finally, the acylthiourea carbonyl is positioned such that attack by the 4-hydroxy group of the *N*-methyl-1,2-benzothiazin 1,1-dioxide ring occurs (see Figure 8). Such ring formation was readily observed for meloxicam (i.e., metabolite M5), but was only seen in trace amounts in sudoxicam incubations. A corresponding cyclized pyrimidinedione (hydrolysis of the thiourea to a urea) metabolite of meloxicam has been reported in vivo in the rat (*15*). It is of interest to note that such a cyclization has never been reported with sudoxicam. Reasons for this are not clear at present time, since both form the acylthiourea (S3/M3), and when isolated, the acylthiourea was shown to spontaneously undergo this ring closing, especially under weakly alkaline conditions. Likewise, the formation of metabolite M6 was interesting in that the molecular weight was consistent with meloxicam monohydroxylation but exact mass measurements on the major fragment ion at *m*/*z* 307 was consistent with a structure derived from the loss of HSCN. A mechanism that accounts for the formation of M6 is shown in Figure 8 and involves initial ring scission of the thiazole epoxide to yield the imino-carbonyl intermediate followed by intramolecular condensation between the carbonyl group with the amide nitrogen to afford the cyclized 2-thioxo-5-hydroxydihydroimidazole metabolite product. While the driving force (enzymatic or chemical) for the cyclization step involving the weak nucleophilic amide nitrogen and an equally weak carbonyl electrophile remains unclear, a rearrangement of similar nature has also been described by Singh et al. in their studies on the bioactivation of a pyrazinone derivative (*24*).

As such, a simple comparison of covalent binding of the two NSAIDs would suggest that meloxicam would likely to be more toxic than sudoxicam. However, several factors are likely to offset these findings. First, in contrast with the exclusive thiazole ring scission pathway observed with sudoxicam, meloxicam metabolism is split between 5-methylthiazolyl hydroxylation (*major pathway leading to detoxication*) and thiazole ring scission (*minor pathway leading to bioactivation*). The existence of a parallel detoxication pathway and the fact that the daily dose of meloxicam (15 mg) is 3-fold lower than that of sudoxicam (45 mg) suggests that the total body burden to reactive acylthiourea metabolite exposure is likely to be considerably less for meloxicam compared with sudoxicam, and may not exceed a threshold needed for eliciting a toxicological response. Second, GSH causes a greater reduction in binding for meloxicam than sudoxicam. Formation of M7 in the presence of GSH may represent a diverting metabolic pathway from bioactivation for meloxicam. Thus, the role of GSH, not as a nucleophilic trapping agent, but rather as a source of reducing equivalents appears to be important in both the metabolism of meloxicam and abating its potential to covalently bind to proteins. Finally, it is also possible that the difference in toxicity observed with the NSAIDs may arise due to the differences in the target macromolecule(s) susceptible to covalent modification. Certainly, this has been demonstrated with 3-hydroxyacetanilide,

an acetaminophen analog, which despite covalently binding to microsomal proteins, is devoid of the hepatotoxic effects associated with acetaminophen (*25, 26*). Therefore, an understanding of adducted macromolecular targets and their roles in modulating essential cellular processes may provide greater insight into mechanisms of toxicity of sudoxicam.

References

(1) Marnett, L. J., Rowlinson, S. W., Goodwin, D. C., Kalgutkar, A. S., and Lanzo, C. A. (1999) Arachidonic acid oxygenation by COX-1 and COX-2. Mechanisms of catalysis and inhibition. *J. Biol. Chem. 274*, 22903–22906.

(2) Rowlinson, S. W., Kiefer, J. R., Prusakiewicz, J. J., Pawlitz, J. L., Kozak, K. R., Kalgutkar, A. S., Stallings, W. C., Kurumbail, R. G., and Marnett, L. J. (2003) A novel mechanism of cyclooxygenase-2 inhibition involving interactions with Ser-530 and Tyr-385. *J. Biol. Chem. 278*, 45763–45769.

(3) Wiseman, E. H., and Chiaini, J. (1972) Anti-inflammatory and pharmacokinetic properties of sudoxicam N-(2-thiazolyl)-4-hydroxy-2-methyl-2H-1,2-benzothiazine-3-carboxamide 1,1-dioxide. *Biochem. Pharmacol. 21*, 2323–2334.

(4) Lombardino, J. G., and Wiseman, E. H. (1972) Sudoxicam and related N-heterocyclic carboxamides of 4-hydroxy-2H-1,2-benzothiazine 1,1-dioxide. Potent nonsteroidal antiinflammatory agents. *J. Med. Chem. 15*, 848–849.

(5) Roth, S. H. (2001) Arthritis therapy: a better time, a better day. *Rheumatology 40*, 603–606.

(6) Rostom, A., Goldkind, L., and Laine, L. (2005) Nonsteroidal anti-inflammatory drugs and hepatic toxicity: a systematic review of randomized controlled trials in arthritis patients. *Clin. Gastroent. Hepatol. 3*, 489–498.

(7) Hobbs, D. C., and Twomey, T. M. (1977) Metabolism of sudoxicam by the rat, dog, and monkey. *Drug Metab. Dispos. 5*, 75–81.

(8) Mizutani, T., Yoshida, K., and Kawazoe, S. (1994) Formation of toxic metabolites from thiabendazole and other thiazoles in mice. Identification of thioamides as ring cleavage products. *Drug Metab. Dispos. 22*, 750–755.

(9) Mizutani, T., and Suzuki, K. (1996) Relative hepatotoxicity of 2-(substituted phenyl)thiazoles and substituted thiobenzamides in mice: evidence for the involvement of thiobenzamides as ring cleavage metabolites in the hepatotoxicity of 2-phenylthiazoles. *Toxicol. Lett. 85*, 101–105.

(10) Dalvie, D. K., Kalgutkar, A. S., Khojasteh-Bakht, S. C., Obach, R. S., and O'Donnell, J. P. (2002) Biotransformation reactions of five-membered aromatic heterocyclic rings. *Chem. Res. Toxicol. 15*, 269–299.

(11) Kalgutkar, A. S., Gardner, I., Obach, R. S., Shaffer, C. L., Callegari, E., Henne, K. R., Mutlib, A. E., Dalvie, D. K., Lee, J. S., Nakai, Y., O'Donnell, J. P., Boer, J., and Harriman, S. P. (2005) A comprehensive listing of bioactivation pathways of organic functional groups. *Curr. Drug Metab. 6*, 161–225.

(12) Stevens, G. J., Hitchcock, K., Wang, Y. K., Coppola, G. M., Versace, R. W., Chin, J. A., Shapiro, M., Suwanrumpha, S., and Mangold, B. L. (1997) In vitro metabolism of N-(5-chloro-2-methylphenyl)-N′-(2-methylpropyl)thiourea: species comparison and identification of a novel thiocarbamide-glutathione adduct. *Chem. Res. Toxicol. 10*, 733–741.

(13) Ji, T., Ikehata, K., Koen, Y. M., Esch, S. W., Williams, T. D., and Hanzlik, R. P. (2007) Covalent modification of microsomal lipids by thiobenzamide metabolites in vivo. *Chem. Res. Toxicol. 20*, 701–708.

(14) Schmid, J., Busch, U., Heinzel, G., Bozler, G., Kaschke, S., and Kummer, M. (1995) Meloxicam. Pharmacokinetics and metabolic pattern after intravenous infusion and oral administration to healthy subjects. *Drug Metab. Dispos. 23*, 1206–1213.

(15) Schmid, J., Busch, U., Trummlitz, G., Prox, A., Kaschke, S., and Wachsmuth, H. (1995) Meloxicam: metabolic profile and biotransformation products in the rat. *Xenobiotica 25*, 1219–1236.

(16) Chesne, C., Guyomard, C., Guillouzo, A., Schmid, J., Ludwig, E., and Sauter, T. (1998) Metabolism of Meloxicam in human liver involves cytochromes P4502C9 and 3A4. *Xenobiotica 28*, 1–13.

(17) Hanzlik, R. P., Cashman, J. R., and Traiger, G. J. (1980) Relative hepatotoxicity of substituted thiobenzamides and thiobenzamide-S-oxides in the rat. *Toxicol. Appl. Pharmacol. 55*, 260–272.

(18) Obach, R. S., Kalgutkar, A. S., Soglia, J. R., and Zhao, S. X. Muraoka, S., and Miura, T. (2008) Can in vitro metabolism-dependent covalent binding data in liver microsomes distinguish hepatotoxic from non-hepatotoxic drugs? An analysis of eighteen drugs with consideration of intrinsic clearance and daily dose. *Chem. Res. Toxicol.*, in press.

(19) Ziegler, D. M. (1978) Intermediate metabolites of thiocarbamides, thioureylenes and thioamides: mechanism of formation and reactivity. *Biochem. Soc. Trans. 6*, 94–96.

(20) Ziegler-Skylakakis, K., Nill, S., Pan, J. F., and Andrae, U. (1998) S-oxygenation of thiourea results in the formation of genotoxic products. *Environ. Mol. Mutagen 31*, 362–373.

(21) Mizutani, T., Ito, K., Nomura, H., and Nakanishi, K. (1990) Nephrotoxicity of thiabendazole in mice depleted of glutathione by treatment with DL-buthionine sulphoximine. *Food Chem. Toxicol. 28*, 169–177.

(22) Mizutani, T., Yoshida, K., and Kawazoe, S. (1993) Possible role of thioformamide as a proximate toxicant in the nephrotoxicity of thiabendazole and related thiazoles in glutathione-depleted mice: structure-toxicity and metabolic studies. *Chem. Res. Toxicol. 6*, 174–179.

(23) Busch, U., Schmid, J., Heinzel, G., Schmaus, H., Baier, J., Huber, C., and Roth, W. (1998) Pharmacokinetics of meloxicam in animals and the relevance to humans. *Drug Metab. Dispos. 26*, 576–584.

(24) Singh, R., Silva Elipe, M. V., Pearson, P. G., Arison, B. H., Wong, B. K., White, R., Yu, X., Burgey, C. S., Lin, J. H., and Baillie, T. A. (2003) Metabolic activation of a pyrazinone-containing thrombin inhibitor. Evidence for novel biotransformation involving pyrazinone ring oxidation, rearrangement, and covalent binding to proteins. *Chem. Res. Toxicol. 16*, 198–207.

(25) Streeter, A. J., Bjorge, S. M., Axworthy, D. B., Nelson, S. D., and Baillie, T. A. (1984) The microsomal metabolism and site of covalent binding to protein of 3′-hydroxyacetanilide, a nonhepatotoxic positional isomer of acetaminophen. *Drug Metab. Dispos. 12*, 565–576.

(26) Myers, T. G., Dietz, E. C., Anderson, N. L., Khairallah, E. A., Cohen, S. D., and Nelson, S. D. (1995) A comparative study of mouse liver proteins arylated by reactive metabolites of acetaminophen and its nonhepatotoxic regioisomer, 3′-hydroxyacetanilide. *Chem. Res. Toxicol. 8*, 403–413.

TX800185B